3-2013

Millimeter-wave phase shifter based on waveguide-mounted RF-MEMS

Dimitra Psychogiou
Swiss Federal Institute of Technology Zurich

Yunjia Li
Swiss Federal Institute of Technology Zurich

Jan Hesselbarth
University of Stuttgart

Stephane Kuehne
Swiss Federal Institute of Technology Zurich

Dimitrios Peroulis
Birck Nanotechnology Center, Purdue University, dperouli@purdue.edu

See next page for additional authors

Psychogiou, Dimitra; Li, Yunjia; Hesselbarth, Jan; Kuehne, Stephane; Peroulis, Dimitrios; Hierold, Christofer; and Hafner, Christian, "Millimeter-wave phase shifter based on waveguide-mounted RF-MEMS" (2013). *Birck and NCN Publications.* Paper 1352.
http://dx.doi.org/10.1002/mop.27390

Authors
Dimitra Psychogiou, Yunjia Li, Jan Hesselbarth, Stephane Kuehne, Dimitrios Peroulis, Christofer Hierold, and Christian Hafner

4. H. Lee, J. Xiong, and S. He, A compact planar MIMO antenna system of four elements with similar radiation characteristics and isolation structure, IEEE Antennas Wireless Propag Lett 8 (2009), 1107–1110.
5. T.S.P. See, Z.N. Chen, and X. Qing, An ultrawideband diversity antenna, IEEE Trans Antennas Propag 57 (2009), 1279–1282.
6. S. Zhang, Z. Ying, J. Xiong, and S. He, Ultrawideband MIMO/ diversity antennas with a tree-like structure to enhance wideband isolation, IEEE Antennas Wireless Propag Lett 7 (2009), 1107–1110.
7. A. Foudazi, A.R. Mallahzadeh, and S.M.A. Nezhad, A triple-band WLAN/WiMAX printed monopole antenna for MIMO applications, Microwave Opt Technol lett 54 (2012), 1321–1325.
8. S. Cheng, P. Hallbjörner, and A. Rydberg, Printed slot planar inverted cone antenna for ultrawideband applications, IEEE Antennas Wireless Propag Lett 7 (2008), 18–21.
9. A. Dastranj, A. Imani, and M. Naser-Moghadassi, Printed wide-slot antenna for wideband applications, IEEE Trans Antennas Propag 56 (2008), 3097–3102.
10. B.S. Yildirim, B.A. Cetiner, G. Roquetra, and L. Jofre, Integrated bluetooth and UWB antenna, IEEE Antennas Wireless Propag Lett 8 (2009), 149–152.
11. A. Foudazi, H.R. Hassani, and S.M.A. Nezhad, A dual-band WLAN/UWB printed wide slot antenna, In: IEEE Loughborough Antennas and Propagation Conference (LAPC), 2011.

MILLIMETER-WAVE PHASE SHIFTER BASED ON WAVEGUIDE-MOUNTED RF-MEMS

Dimitra Psychogiou,[1] Yunjia Li,[2] Jan Hesselbarth,[3] Stephane Kühne,[2] Dimitrios Peroulis,[4] Christofer Hierold,[2] and Christian Hafner[1]
[1] Laboratory for Electromagnetic Fields and Microwave Electronics, Department of Information Technology and Electrical Engineering, ETH Zurich, 8092 Zürich, Switzerland; Corresponding author: pdimitra@ifh.ee.ethz.ch
[2] Group of Micro and Nanosystems, Department of Mechanical and Process Engineering, ETH Zurich, 8092 Zürich, Switzerland
[3] Institute of Radio Frequency Technology, University of Stuttgart, Stuttgart 70569, Germany
[4] Birck Nanotechnology Center, School of Electrical and Computer Engineering, Purdue University, West Lafayette, IN 47907

Received 11 June 2012

ABSTRACT: *A continuously variable transmission type W-band phase shifter based on a single pole bandpass filter tuned by MEMS actuated fingers is reported. Tuning is achieved by means of two half-wavelength long conductive fingers that synchronously rotate upwards in an antiparallel fashion. The fingers deflection results in a distributed variable shunt capacitance which in turn leads to a variable analog phase shift. For an applied DC bias voltage between 0 and 26 V, the transmission phase can be continuously varied up to 46.4° at a frequency of 106 GHz with an insertion loss of less than 3.4 dB.* © 2012 Wiley Periodicals, Inc. Microwave Opt Technol Lett 54:465–468, 2013; View this article online at wileyonlinelibrary.com. DOI 10.1002/mop.27390

Key words: *phase shifter; RF-MEMS; resonator; analog tuning*

1. INTRODUCTION

Recent advances in imaging, radar and sensing systems have imposed the design of low loss, high-performing phase shifters for frequencies between 75 and 110 GHz commonly known as W-band. Millimeter-wave phase shifters are fundamental components of beamforming and phased antenna arrays intended to be used for automotive anticollision radar, weather monitoring, and medical imaging applications.

Topologies presented in the literature are mainly based on MEMS-switched true-time delay-lines or periodically capacitive-loaded transmission lines [1, 2]. In an alternative way, materials with tunable characteristics such as ferrites or ferroelectrics are used [3]. The first approach is often suitable for applications that require discrete phase shift variations. It requires a large number of tuning elements and is limited by high dissipation loss and low power handling. The second approach leads to bulky devices prone to excessive dissipated power due to the high dielectric losses of the involved materials and requires high power for operation.

For frequencies beyond a few GHz, air-filled metal waveguides outperform planar transmission lines in terms of low loss and high-power handling [4]. If used in combination with tunable components such as MEMS, they may pave the way to outperforming reconfigurable devices. An example of this approach was shown in Ref. 5 where a MEMS-based high impedance surface was used as a tunable back-short of a reflective-type phase shifter.

In this article, an analog transmission-type phase shifter based on MEMS tilting fingers [6] integrated beneath a half-wavelength long ridge waveguide resonator is presented. A prototype for frequencies between 96 and 106 GHz has been designed, manufactured, and experimentally validated.

2. PHASE SHIFTER CONCEPT

The proposed phase shifter concept is based on a single pole bandpass filter tuned around its center frequency by a single distributed shunt capacitance which results in a variation of the transmission phase. The maximum achievable phase shift is limited by the available variation of the capacitive loading and by the deterioration of the input reflection occurring at both minimum and maximum loading states. A realization concept of the phase shifter includes a low-impedance half-wavelength long ridge waveguide section and a MEMS chip with a pair of electrostatically actuated fingers, mounted inside the waveguide bottom wall (Fig. 1). The two sets of conductive fingers are either set flat in parallel with the waveguide bottom wall or synchronously rotate in an antiparallel fashion out of the bottom wall plane and toward the ridge (Fig. 2). Considering the length of the fingers of almost half a guided wavelength long, this rotational movement realizes a variable distributed shunt capacitance in the waveguide. For a design frequency around 100 GHz, the cross-sectional dimensions of the waveguide are: width: 1.5 mm, height: 1 mm, ridge width: 0.6 mm, ridge height: 0.5 mm. The low-impedance ridge has a height of 0.8 mm and the dimensions of the MEMS fingers are: length 1.4 mm and width 0.15 and 0.3 mm for the center finger and the edge fingers, respectively.

3. RF-MEMS CHIP

For the RF-MEMS chip design, a tilting micromirror approach is followed (Fig. 3). It is based on electrostatic actuation and features a torsional out-of-plane-modus of movement. Basic design and technology aspects have been presented in Ref. 7 and modified for the particular application. To achieve the high static deflection angle between 0 and 7.5° (g: 0–168 μm, h: 200–32 μm) with a low DC actuation voltage (<27.5 V), a soft SU8 polymer spring has been integrated underneath each torsional bar. The fabrication process is based on a bulk silicon micromachining process as described in Ref. 7. The chip is composed of a stack of three double-side polished monocrystalline silicon wafers (thickness: device layer 80 μm, stator layer

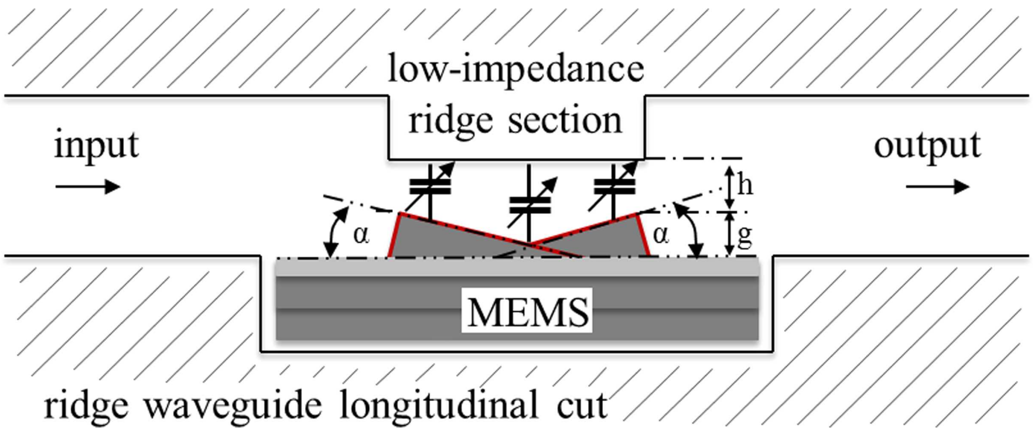

Figure 1 Concept of a waveguide-mounted RF-MEMS phase shifter: longitudinal cut through the ridge waveguide and the MEMS chip. [Color figure can be viewed in the online issue, which is available at wileyonlinelibrary.com]

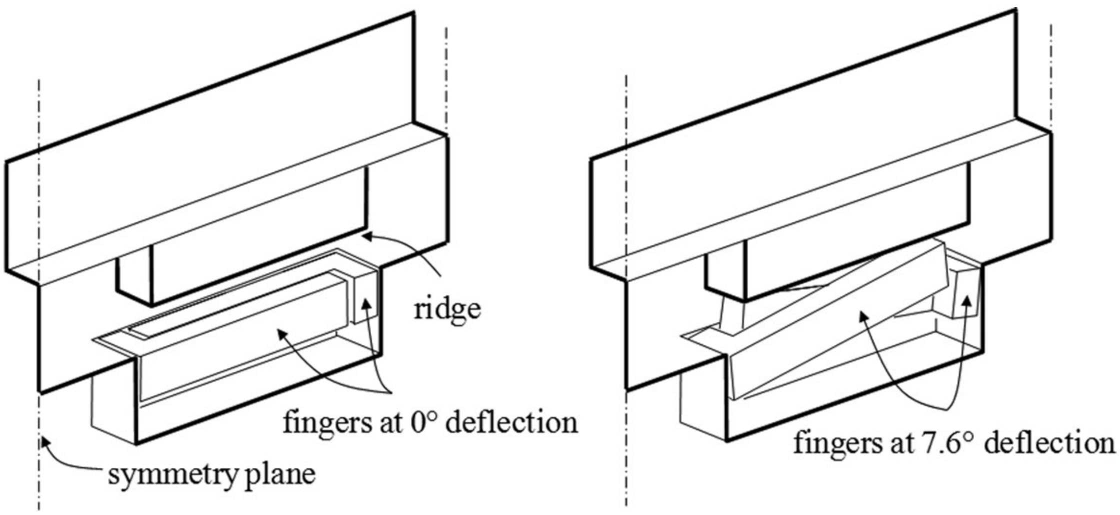

Figure 2 Detailed view of two different deflection states of the MEMS actuated fingers positioned beneath the ridge waveguide resonator: MEMS fingers at 0° deflection (left), MEMS fingers at 7.6° deflection (right)

180 μm, handle layer 400 μm) and a top metallization layer of 500 nm Au. As the device layer including the moving fingers is in direct contact with the RF signal path, a low resistivity silicon wafer with $\rho < 0.001$ Ω·cm and a top metallization layer is used for the device layer to reduce the RF loss. For both stator and handle layer wafers with resistivity ρ 1–10 Ω·cm are used.

4. RESULTS

Figure 4 illustrates the manufactured waveguide fixture for the continuously variable phase shifter. It is based on a split-block approach and was made by high precision milling and electron discharge machining. The chip is first glued on a 5 mil RT Duroid 5880 substrate and wire-bonded to the external DC biasing lines. The substrate is then mounted on the bottom part of the fixture and centred via optical alignment.

Figure 5 depicts the calibration curves of the fingers static deflection as a function of the applied DC bias voltage for one MEMS device characterized by a white light interferometer prior to the RF measurement (fast measurement cycle). The indicated nine biasing states correspond to the equal angles for both fingers applied for the phase shifter characterization. A maximum deflection angle of 7.6° was achieved with an actuation voltage of 26 V. The slightly different actuation characteristics of the two fingers as well as the −0.1° initial tilt is due to device asymmetries and fabrication related geometry variations. The one-sided error bars in Figure 5 indicate the typical angle uncertainty (systematic error) due to the viscoelastic properties of the SU-8 springs, which has been determined with a test

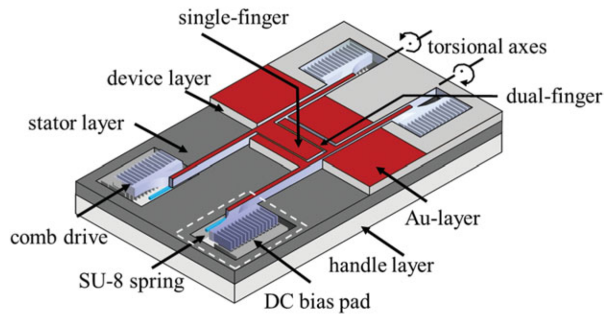

Figure 3 Schematic illustration of the dual-axis tilting micromirror MEMS chip. [Color figure can be viewed in the online issue, which is available at wileyonlinelibrary.com]

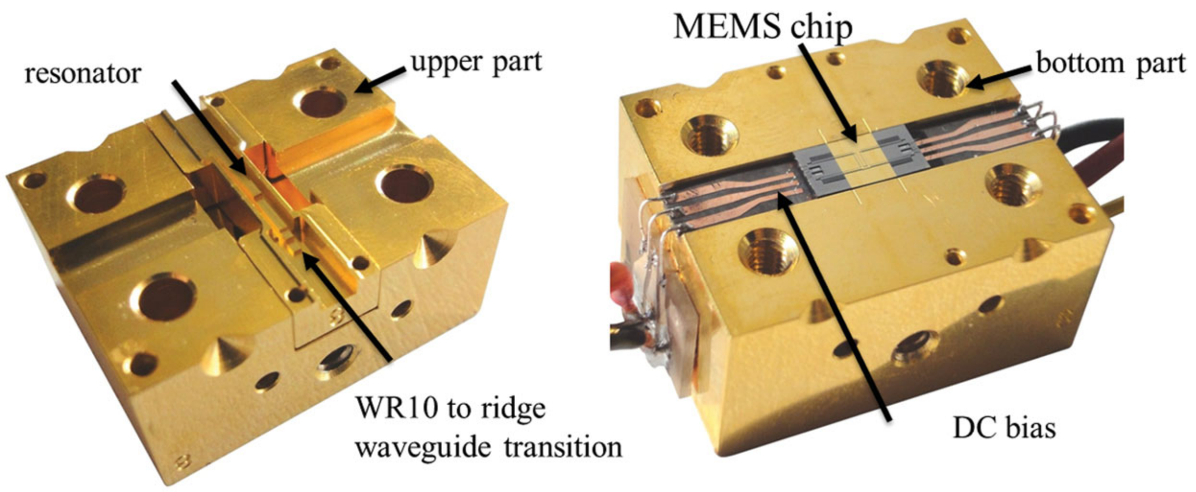

Figure 4 Manufactured phase shifter: upper part showing the half-wavelength long ridge waveguide. Resonator and two WR10 to ridge waveguide transitions (left), bottom part showing the RF-MEMS chip integrated in the waveguide bottom wall (right). [Color figure can be viewed in the online issue, which is available at wileyonlinelibrary.com]

device and a spring of the same geometry starting with high deflection angles at point 1 (Fig. 5). The error develops, therefore, as indicated toward smaller angles due to the limited resting/measurement time of 200 s and the varying load conditions.

The manufactured phase shifter was measured with an Agilent 8510 network analyzer with calibration planes defined at the waveguide flanges. The worst-case input reflection for different bias states is below -10 dB in the frequency range between 96 and 106 GHz. For this frequency range, the transmission phase measured at various DC bias states (states 1–9, as illustrated in Fig. 5) is shown in Figure 6. The transmission phase at zero bias voltage has been subtracted from these measurements so as to better illustrate the phase variation range that grows from 22.4° at 96 GHz to 46.4° at 106 GHz. Figure 7 shows the transmission loss measured at various DC biasing states. The insertion loss of the WR10 to a ridge waveguide transition was measured around 0.23 dB back-to-back with a separate fixture and is de-embedded from these measurements. At 106 GHz, the maximum phase variation is 46.4°, causing an insertion loss of 3.4 dB. This corresponds to a maximum figure of merit (FOM) of 13.6°/dB. The measured phase shift variation range is in good agreement with the simulated phase shift variation range (obtained by finite element solver, HFSS) for variable MEMS fingers deflections (α) between $-0.1°$ and 7.6° or capacitive gap variations (h) between 25 and 200 μm and it grows from 24° at 96 GHz to 46° at 106 GHz.

The increase of insertion loss with deflection angle (Fig. 7) can be attributed to increased conductive losses caused by the large surface current density for smaller capacitive gaps. In addition, when the MEMS fingers are positioned at high deflection states, the current leakage to the MEMS substrate increases due to an opened air cavity below the MEMS fingers. Such a cavity acts as a discontinuity and allows the current to flow in

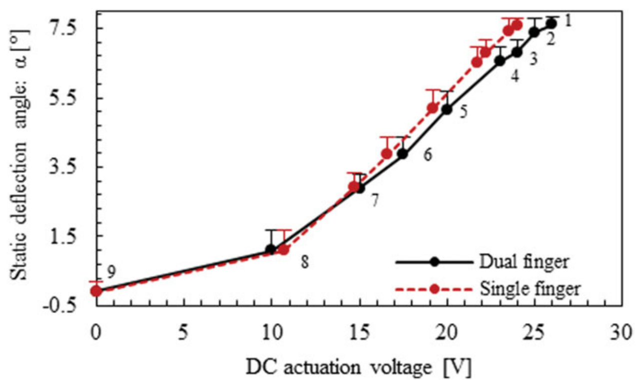

Figure 5 Measured deflection angle of the MEMS actuated fingers under various DC biasing voltages. [Color figure can be viewed in the online issue, which is available at wileyonlinelibrary.com]

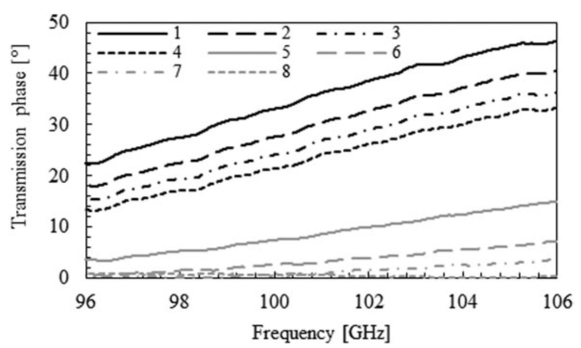

Figure 6 Measured transmission phase shift for various DC biasing voltages (DC biasing states: 1–9, as shown in Fig. 5) using the zero bias state (9) as a reference phase

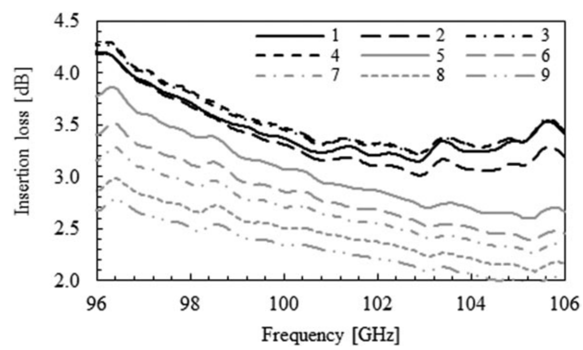

Figure 7 Measured insertion loss under various DC biasing voltages (DC biasing states: 1–9, as shown in Fig. 5)

the stator and handle layer which are made out of lossy silicon (ρ: 1–10 Ω·cm) and therefore create additional loss.

5. CONCLUSION

A continuously variable transmission type phase shifter based on a single-pole bandpass filter and MEMS actuated fingers is presented. For an applied DC bias voltage between 0 and 26 V, the proposed device realizes a continuously variable phase shift between 0 and 46.4° at 106 GHz while having an insertion loss of less than 3.4 dB, corresponding to a maximum FOM of 13.6°/dB.

ACKNOWLEDGMENTS

This work has been supported by the Swiss National Science Foundation (SNF) under grant 200021_129832. The authors would like to thank C. Maccio, H.-R. Benedickter and M. Lanz for their technical support.

REFERENCES

1. A. Stehle, G. Georgiev, V. Ziegler, B. Schoenlinner, U. Prechtel, H. Seidel, and U. Schmid, RF-MEMS switch and phase shifter optimized for W-band, In: Proceedings European Microwave Conference, Amsterdam, 2008, pp. 104–107.
2. J.-J. Hung, L. Dussopt, and G.M. Rebeiz, Distributed 2- and 3-bit W-band phase shifters on glass substrates, IEEE Trans Microwave Theory Tech 52 (2004), 600–606.
3. M.A. Popov, I.V. Zavislyak, and G. Srinivasan, Magnetic field tunable 75–110 GHz dielectric phase shifter, Electron Lett 46 (2010), 569–570.
4. M. Daneshmand and R.R Mansour, Multi-port MEMS-based waveguide and coaxial switches, IEEE Trans Microwave Theory Tech 53 (2005), 3531–3537.
5. D. Chicherin, M. Sterner, J. Oberhammer, S. Dudorov, J. Aberg, and A.V. Räisänen, Analog type millimeter wave phase shifters based on MEMS tunable high-impedance surface in rectangular metal waveguide, In: IEEE MTT-S International Microwave Symposium Digest, Anaheim, 2010, 61–64.
6. D. Psychogiou, J. Hesselbarth, Y. Li, S. Kühne, and C. Hierold, W-band tunable reflective type phase shifter based on waveguide-mounted RF MEMS, In: IEEE MTT-S International Microwave Workshop Series on Millimeter Wave Integration Technologies, Sitges, 2011, pp. 85–88.
7. Y. Li, S. Kühne, D. Psychogiou, J. Hesselbarth, and C. Hierold, A microdevice with large deflection for variable-ratio RF MEMS power divider applications, J Micromech Microeng 21 (2011), 074013/1–9.

DUAL-BAND VCO WITH COMPOSITE RIGHT-/LEFT-HANDED RESONATOR

Sheng-Lyang Jang, You-Wei Liu, Chia-Wei Chang, and Ching-Wen Hsue
Department of Electronic Engineering, National Taiwan University of Science and Technology, Taipei, Taiwan; Corresponding author: m9502216@mail.ntust.edu.tw

Received 15 June 2012

ABSTRACT: *This article proposes a high-performance CMOS voltage-controlled oscillator (VCO) implemented with composite right-/left-handed nonmobius-connected LC-rings to provide dual-band differential outputs. The VCO consists of two cross-coupled sub-VCOs sharing series-LC resonators. nMOSFET switches are used to control high- and low-band outputs. The proposed VCO has been implemented with the TSMC 0.18 μm SiGe BiCMOS technology. The die area of the VCO is 1.16 × 1.12 mm2. With the switch on, the odd-mode VCO operates at the high-frequency 6 GHz band, and when the switch is off, the even-mode VCO operates at the low-frequency 4 GHz band.* © 2012 Wiley Periodicals, Inc. Microwave Opt Technol Lett 54:468–471, 2013; View this article online at wileyonlinelibrary.com. DOI 10.1002/mop.27375

Key words: *composite right-/left-handed LC network; mode switching; LC resonator; differential dual-band VCOs*

1. INTRODUCTION

Driven by multistandards and multiservices wireless radios, many voltage-controlled oscillator (VCO) dual-band techniques have been presented in recent year to cover the wide spectrum and meet the stringent phase-noise requirement. Traditionally, implementing a frequency source covering a wide range of frequencies can be done by multiplexing several on-chip sources, and this consumes large die area and increases production cost [1]. An alternative approach is to use a single multiband oscillator to cover multiple channels by direct switching of capacitive and inductive components [2, 3], and the parasitic channel resistance in MOSFET switches degrades the Q-factor of LC resonator and the phase noise of VCO. This approach uses a single-resonance resonator, the frequency band changes based on the switching resonator's inductance or capacitance. Alternatively, a dual-band VCO [4] can be implemented with a single negative resistance cell in conjunction with a fourth-order LC resonator with a varactor tuning is used to switch high-/low-frequency band. This approach has no switch loss because it uses no MOSFET switch. The dual-resonance VCO [4, 5] uses a unit of a composite right-/left-handed (CRLH) [6] resonator and has drawback of lower low-band output power than high-band output power.

In this article, a dual-band VCO based on two units of CRLH resonators is presented and is capable of generating unevenly spaced resonant frequencies. The proposed VCO can provide large output power at both low- and high-frequency bands. A CRLH resonator is shown in Figure 1, where a unit cell consists of a series LC branch due to the inductor-varactor pair L_R, and C_L, and a shunt LC branch due to the inductor-varactor pair L_L, and C_R. The implemented VCO was fabricated in the TSMC 0.18 μm SiGe BiCMOS process.

A negative resistance generator in conjunction with a CRLH resonator can be used to form an oscillator. A voltage-tunable passive such as C_R or C_L in the CRLH can be used to control the oscillation frequency for the VCO. For a VCO circuit to oscillate, the total phase shift of one round trip through the non-mobius-connected ring must be equal to $2n\pi$, where $n = 0, \pm1, \pm2, \ldots$ The second condition is that the negative resistance

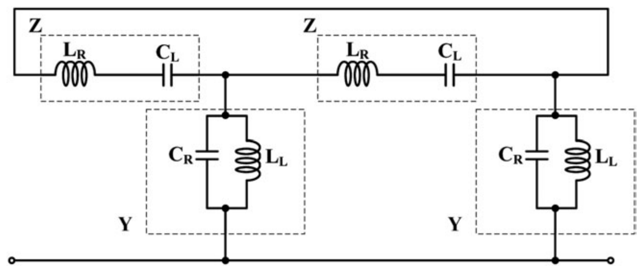

Figure 1 Schematic of the composite right-/left-handed nonmobius-connected ring